# Multi-Look Stripmap SAR Processing Algorithm with Built-In Correction of Geometric Distortions

Oleksandr O. Bezvesilniy, Ievgen M. Gorovyi, Sergiy V. Sosnytskiy, Volodymyr V. Vynogradov, Dmytro M. Vavriv, Department of Microwave Electronics, Institute of Radio Astronomy of NAS of Ukraine, Ukraine

## Abstract

SAR systems installed on small aircrafts suffer from trajectory deviations and instabilities of antenna orientation. These kinds of motion errors lead to significant geometric distortions in SAR images. In the paper, we describe a time-domain multi-look stripmap SAR processing algorithm with built-in correction of geometric distortions. In the algorithm, the azimuth reference functions and range migration curves are specially designed to produce SAR images directly on a correct rectangular grid on the ground plane. The proposed technique has been successfully tested by using a Ku-band airborne SAR system.

## 1 Introduction

The formation of high-quality multi-look SAR images with airborne SAR systems installed on small aircrafts is a difficult problem because of significant motion and orientation errors of such light-weight platforms. Deviations of the aircraft trajectory and instabilities of the antenna orientation lead to geometric and radiometric errors in SAR images [1]-[3].

Geometric distortions in SAR images can be corrected by interpolation of images to a rectangular grid on the ground plane taking into account the measured aircraft trajectory and the orientation of the synthetic aperture beams (SAR beams). However, this approach becomes inefficient in case of significant geometric distortions.

The clutter-lock technique is usually used to avoid radiometric errors in SAR images [4]. According to this technique, the azimuth reference functions are built adaptively to track time variations of the Doppler centroid. However, in case of fast and significant instabilities of the antenna orientation, the clutter-lock technique leads to strong geometric errors in SAR images and should not be used.

Instabilities of the aircraft orientation could be compensated by the antenna stabilization, although it is a complicated and expensive solution. An application of a wide-beam antenna firmly mounted on the aircraft is another way to guarantee the uniform illumination of the ground scene in the center of the antenna spot despite of the instabilities of the platform orientation.

In the paper, we propose a time-domain multi-look stripmap SAR processing algorithm with built-in correction of geometric distortions. In the algorithm, the azimuth reference functions and range migration curves are specially designed to produce SAR images directly on a correct rectangular grid on the ground plane.

The proposed technique does not use the clutter-lock – the orientation of the SAR beams is fixed. As a result, the algorithm works well without an additional radiometric correction only for a wide-beam antenna and for SAR looks which are close to the centre of the antenna beam. Otherwise, some radiometric correction should be applied to the obtained SAR images.

The proposed technique has been successfully tested by using a Ku-band airborne SAR system, installed on a light-weight aircraft [5].

## 2 Time-Domain Convolution-Based SAR Processing

The proposed SAR processing algorithm is based on the one-dimensional time-domain convolution of the signals interpolated from range-compressed data along the migration curves

$$R(\tau) \approx R - \frac{\lambda}{2} F_{DC} \tau - \frac{\lambda}{2} F_{DR} \frac{\tau^2}{2} \qquad (1)$$

with the reference functions

$$h(\tau) = w(\tau) \exp\left[ i \frac{4\pi}{\lambda} R(\tau) \right]. \qquad (2)$$

Here $R(\tau)$ is the slant range to the target, $\lambda$ is the radar wavelength, $w(\tau)$ is the weighting window applied to improve the side-lobe level of the synthetic aperture pattern.

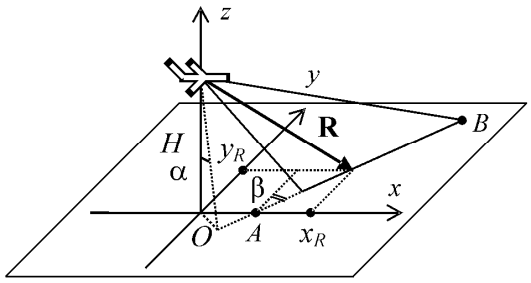


**Figure 1:** Stripmap SAR geometry.

The Doppler centroid $F_{DC}$ and the Doppler rate $F_{DR}$ are given by

$$F_{DC} = \frac{2}{\lambda}\frac{(\vec{\mathbf{R}}\cdot\vec{\mathbf{V}})}{R}, \quad (3)$$

$$F_{DR} = -\frac{2}{\lambda}\left[\frac{V^2}{R}\left(1-\frac{(\vec{\mathbf{R}}\cdot\vec{\mathbf{V}})^2}{R^2V^2}\right)-\frac{(\vec{\mathbf{R}}\cdot\vec{\mathbf{A}})}{R}\right]. \quad (4)$$

Here $\vec{\mathbf{V}}$ and $\vec{\mathbf{A}}$ are the aircraft velocity and acceleration vectors, correspondingly. The slant range vector $\vec{\mathbf{R}} = (x_R, y_R, -H)$ goes from the antenna phase center to the point $(x_R, y_R)$ on the ground at which the synthetic beam will be aimed (**Figure 1**). The $x$-axis of the local coordinate system is pointed along the horizontal component of the aircraft velocity vector (so that $V_y = 0$). The $z$-axis is pointed upward and goes through the antenna phase center. $H$ is the aircraft flight altitude. The point $(x_R, y_R)$ is on the Doppler centroid line $AB$ which is the intersection of the elevation plane of the real antenna pattern and the ground plane. The orientation of the real antenna is described by the antenna pitch angle $\alpha$ and the antenna yaw angle $\beta$ so that

$$x_R = H\tan\alpha\cos\beta + \sin\beta\sqrt{R^2-(H/\cos\alpha)^2}, \quad (5)$$

$$y_R = -H\tan\alpha\sin\beta + \cos\beta\sqrt{R^2-(H/\cos\alpha)^2}. \quad (6)$$

The aircraft flight altitude, velocity and acceleration, as well as the antenna beam orientation angles may change slowly but they are assumed to be constant during the time of synthesis.

The azimuth resolution is given by

$$\rho_X = K_w V_X/(|F_{DR}|T_S). \quad (7)$$

The coefficient $K_w$ describes broadening of the main lobe of the synthetic aperture pattern caused by windowing.

The described SAR processing algorithm is effective for building moderate-resolution SAR images when the time-domain convolution is not too long. The advantage of the algorithm is its ability to build each pixel of the SAR image with a particular reference function and migration curve. It means that the algorithm works well for the time-varying and range-dependent Doppler centroid and Doppler rate, which is important for small and light-weight SAR platforms.

# 3 Time-Domain Multi-Look SAR Processing

The multi-look SAR processing is used to suppress speckle noise in SAR images [1], [6] and for other applications, for example, for measuring the Doppler centroid with high accuracy and high spatial resolution [7].

According to the multi-look processing, the whole azimuth Doppler bandwidth

$$\Delta F_{D\max} = F_{DR}T_{S\max} \quad (8)$$

is divided on the sub-bands which may partly overlap. Each sub-band is processed separately in order to form a SAR look image. For half-overlapped sub-bands the central frequencies $F_{DC}(R,n)$ and width $\Delta F_D$ of the sub-bands of the SAR looks are

$$F_{DC}(R,n) = F_{DC}(R) + \Delta F_{DC}(n), \quad (9)$$

$$\Delta F_{DC}(n) = n\frac{\Delta F_D}{2}, \quad (10)$$

$$\Delta F_D = \frac{2\Delta F_{D\max}}{N_L+1}. \quad (11)$$

where $n = -N_L/2, ..., N_L/2-1$ is the SAR look index, $N_L$ is the number of the SAR looks.

The time of synthesis of the SAR look is

$$T_S = \frac{2T_{S\max}}{N_L+1}. \quad (12)$$

Taking into account the relation (7) for the azimuth resolution, the central frequencies of the SAR looks (9) can be written as

$$F_{DC}(R,n) = F_{DC}(R) - n\frac{K_w}{2}\frac{V_X}{\rho_X}. \quad (13)$$

The multi-look processing in time domain is usually based on dividing the reference function built on the whole long interval of synthesis $T_{S\max}$ on several sub-intervals. In this approach we should guarantee that there are no significant uncompensated phase errors during this long coherent processing time.

However, as a matter of fact, in order to achieve the desired azimuth resolution for one SAR look it is sufficient to perform coherent processing on the much shorter time interval $T_S$ (12). Following this idea, we should process the data collected during the time of synthesis $T_S$ with a set of different reference functions to form multi-look SAR beams. The question is how to build the required reference functions.

As it has been shown in the previous section, in order to aim the SAR beam at the point $(x_R, y_R)$ we should perform processing with the corresponding range migration curve (1) and reference function (2) with the Doppler centroid $F_{DC}(R)$ (3) and the Doppler rate $F_{DC}(R)$ (4). The SAR look beam

formed with the central frequency $F_{DC}(R)+\Delta F_{DC}(n)$ (9)-(11) will be pointed to some point $(x_R+\xi_n, y_R+\eta_n)$. What are the coordinates of this point?

First, since the signal from this point has appeared at the slant range $R$ when the aircraft is at the center of the synthetic aperture, we can write:

$$\sqrt{x_R^2+y_R^2+H^2}=\sqrt{(x_R+\xi_n)^2+(y_R+\eta_n)^2+H^2},$$
$$x_R^2+y_R^2=(x_R+\xi_n)^2+(y_R+\eta_n)^2. \quad (14)$$

Second, the position of the point in azimuth direction is related to its Doppler centroid (3), so we can write

$$F_{DC}(R)+\Delta F_{DC}(n)=\frac{2}{\lambda}\frac{(x_R+\xi_n)V_X-HV_Z}{R},$$
$$\Delta F_{DC}(n)=\frac{2}{\lambda}\frac{V_X}{R}\xi_n. \quad (15)$$

Thus, in order to form the set of SAR looks for slant range $R$ we should first calculate the corresponding points $(x_R+\xi_n, y_R+\eta_n)$ on the ground from (14) and (15) and then process the same raw data on the interval of synthesis $T_S$ with the appropriate range migration curves (1) and reference functions (2) with Doppler centroid (3) and Doppler rate (4).

It should be noted here that SAR beams of different looks are aimed at different points on the ground. It means that SAR look images are sampled on different grids. Therefore, SAR look images should be first re-sampled to the same ground grid and only then they can be averaged to produce the multi-look image. The deviations of the aircraft trajectory introduce further complexity into the re-sampling process. An efficient approach to solve this problem called "built-in correction of geometric distortions" is proposed in the next section.

# 4 Built-In Correction of Geometric Distortions

The idea of the built-in correction of geometric distortions is to point the SAR beams exactly to the nodes of the rectangular grid on the ground plane. The algorithm consists of the following steps. First, we should specify the reference flight trajectory with the constant aircraft flight altitude $H_0$, velocity $V_0$, and the pulse repetition period $T_0$, as well as the reference orientation of the antenna beam with the constant antenna pitch and yaw angles $\alpha_0$ and $\beta_0$. These reference parameters are used to calculate the time-independent Doppler centroid $F_{DC}(R)$, the central Doppler frequencies of the SAR looks $F_{DC}(R)+\Delta F_{DC}(n)$, and the coordinates of the reference points on the ground plane, to which the SAR look beams should be pointed:

$$x_{ref}(n,R),\ y_{ref}(n,R). \quad (16)$$

After that we should find the nodes of the correct rectangular grid on the ground, which are close to these points (by using interpolation):

$$x_{ref}^{node}(n,i_Y),\ y_{ref}^{node}(n,i_Y). \quad (17)$$

Here $i_Y$ is the in ground range index of the grid.

There are two important requirements for the azimuth grid step $\Delta x$. First, the grid step must be multiple of the pulse repetition path:

$$\Delta x=k_\Delta V_0 T_0, \quad (18)$$

where $k_\Delta$ is an integer number. Second, there must be at least one sample per resolution cell:

$$\Delta x=\rho_x/k_s,\ k_s\ge 1. \quad (19)$$

Typically, the sampling factor is chosen to be $k_s\approx 2$ (two samples per resolution cell). If the coordinates of the nodes of the adjacent looks $x_{ref}^{node}(n,i_Y)$ and $x_{ref}^{node}(n+1,i_Y)$ are closer than the grid step $\Delta x$, these nodes will coincide. To prevent such situation we should decrease the grid step $\Delta x$ and, consequently, increase the sampling factor $k_s$.

Finally, in order to produce geometrically correct SAR images we should point the synthetic beams to the corresponding nodes:

$$x_{ref}^{node}(n,i_Y)+i_X\Delta x,\ y_{ref}^{node}(n,i_Y). \quad (20)$$

To do this, we should transform the coordinates of these nodes from the reference local coordinate system to the actual local coordinate system taking into account actual aircraft position and orientation of the velocity vector. Thus, we obtain SAR image samples $SAR(n,i_X,i_Y)$ in the nodes $(i_X,i_Y)$ of the rectangular grid of the ground plane.

# 5 Experimental Results

The proposed algorithm with the built-in geometric correction has been tested by using a Ku-band airborne SAR system, installed on a light-weight aircraft [5].

The left SAR image in **Figure 2** is built by using the clutter-lock. One can see geometric distortions caused by instabilities of the antenna orientation. The right SAR image is formed by using the built-in geometric correction. Both images have 3-m resolution and are built by using 3 looks.

The accuracy of the geometric correction is illustrated in **Figure 3**, where the SAR image composed of 45 looks and formed by using the built-in geometric correction is imposed on the Google Map image of the scene.

One can see that the proposed algorithm with built-in correction of geometric distortions allows us to obtain high-quality multi-look SAR images.

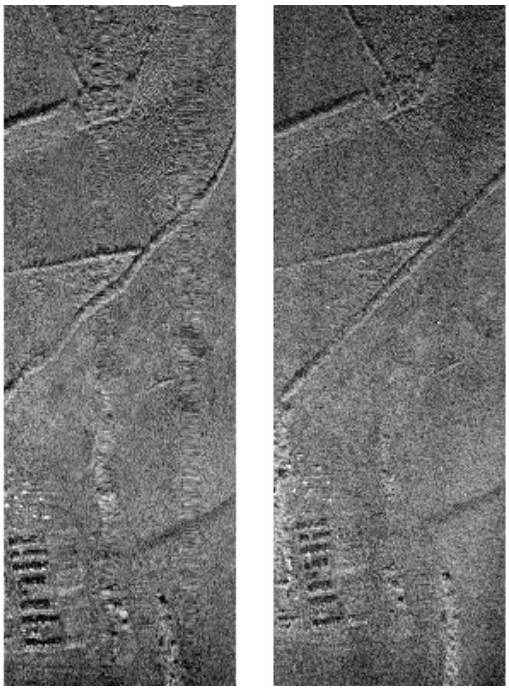

**Figure 2:** The left SAR image is built by using the clutter-lock. The right SAR image is formed by using the built-in geometric correction.

**Figure 3:** The 45-look SAR image formed by using the built-in geometric correction is imposed on the Google Map image of the scene.

# 6 Conclusion

Pros of the proposed algorithms:

1. No additional interpolation of SAR images is required. SAR images are already geometrically correct after synthesis.
2. Reduced requirements to motion compensation. Trajectory deviations should be measured and compensated with the high accuracy of a fraction of the radar wavelength only during the time of synthesis of one look (0.25 s for 3-m resolution). In order to build the multi-look image, the trajectory should be measured with the accuracy of a fraction of the SAR resolution during the time of data acquisition for all looks (5.6 s for 45 looks).
3. Operation from light-weight aircraft platforms with a non-stabilized or fixed-mounted antenna.
4. Operation with a less expensive navigation system since orientation measurements are not required.

Cons of the proposed algorithms:

1. Lots of computations in case of SAR imaging with very high resolution because of the long time-domain convolution.
2. Other SAR processing methods are more efficient if the SAR system is equipped with a stabilized antenna and a good navigation system, and full motion compensation is performed.

# References


[1] Oliver C.J., Quegan S. *Understanding Synthetic Aperture Radar Images.* Boston; London: Artech House, 1998.

[2] Buckreuss S. *Motion errors in an airborne synthetic aperture radar system*, European Trans. on Telecommunication, Vol. 2, No. 6, pp. 655-664, 1991.

[3] Blacknell D. et al., *Geometric accuracy in airborne SAR images*, IEEE Trans. on Aerospace and Electronic Systems, vol. 25, no. 2, pp. 241-258, March 1989.

[4] Madsen S. N.: *Estimating the Doppler centroid of SAR data*, IEEE Trans. Aerospace and Electronic Systems, vol. 25, no. 2, pp. 134-140, March 1989.

[5] Vavriv D.M. et al., *Cost-effective Ku-band airborne SAR with Doppler centroid estimation, autofocusing and indication of moving targets*, Proc. 2nd European Radar Conf. EuRAD2005, Paris, France, pp. 21-24.

[6] Moreira A., *Improved multilook techniques applied to SAR and SCANSAR imagery*, IEEE Trans. on Geoscience and Remote Sensing, vol. 29, no. 4, pp. 529-534, July 1991.

[7] Bezvesilniy O.O., Dukhopelnykova I.V., Vinogradov V.V., Vavriv D.M., *Retrieving 3-D topography by using a single-antenna squint-mode airborne SAR*, IEEE Trans. on Geoscience and Remote Sensing, vol. 45, no. 11, pp. 3574-3582, November 2007.